

Recommendations to address uncertainties in environmental risk assessment using toxicokinetics-toxicodynamics models

Virgile Baudrot^{1*} and Sandrine Charles¹

¹Univ Lyon, Université Lyon 1, UMR CNRS 5558, Laboratoire de Biométrie et Biologie Évolutive, F-69100 Villeurbanne, France

Abstract

Providing reliable environmental quality standards (EQS) is a challenging issue for environmental risk assessment (ERA). These EQS are derived from toxicity endpoints estimated from dose-response models to identify and characterize the environmental hazard of chemical compounds as those released by human activities. The classical toxicity endpoints are the $x\%$ effect/lethal concentrations at a specific time t ($EC/LC(x, t)$), or the multiplication factors applied to environmental exposure profiles leading to $x\%$ of effect reduction at a specific time t ($MF(x, t)$). However, classical dose-response models used to estimate the toxicity endpoints have some weaknesses such as their dependency on observation time-points which are likely to differ between species. Also, real exposure profiles are hardly ever constant over time, what makes impossible the use of classical dose-response models and compromises the derivation of $MF(x, t)$, actually designed to tackle time-variable exposure profiles. When dealing with survival or immobility toxicity test data, these issues can be overcome with the use of the General Unified Threshold model of Survival (GUTS), a toxicokinetics-toxicodynamics (TKTD) model, providing an explicit framework to analyse both time and concentration-dependent data sets, as well as a mechanistic derivation of $EC/LC(x, t)$ and $MF(x, t)$ whatever x and at any time t of interest. In addition, the assessment of a risk is inherently built upon probability distributions, so that the next critical step for ERA is to characterize uncertainties of toxicity endpoints, and sequentially of EQS. The innovative approach investigated in our paper is the use of the Bayesian framework to deal with uncertainties arising in the calibration process and propagated all along the successive prediction steps until the $LC(x, t)$ and $MF(x, t)$ derivations. We also explored the mathematical properties of $LC(x, t)$ and $MF(x, t)$ as well as the impact of different experimental designs in order to provide some recommendations for a robust derivation of toxicity endpoints leading to reliable EQS.

Keywords. Survival models ; Dose-Response ; GUTS ; Lethal Concentration ; Multiplication Factor ; Margin of safety ; Environmental Risk Assessment

1. Introduction

Assessing the environmental risk of chemical compounds requires environmental quality standards (EQS) such as PNECs, RACs and MAC-EQS under the ECHA, EFSA PPR and WFP regulatory

33 frameworks respectively (EFSA PPR, 2013; ECHA, 2017). Derivation of EQS results from the com-
34 bination of assessment factors with toxicity endpoints mainly derivated from estimated or measured
35 exposure response of a set of target species to that chemical compound (EFSA PPR, 2013; Isigonis
36 et al., 2015; Syberg and Hansen, 2016; ECHA, 2017). Deriving reliable toxicity endpoints is challenging
37 and the subject matter is very controversial (Laskowski, 1995; Jager, 2011). Today, Environmental
38 Risk Assessment (ERA) rests on fitting classical dose-response models to quantitative toxicity test
39 data. For acute effect assessment, such data are collected from standard toxicity tests, from which the
40 50% lethal or effective concentration (LC_{50} or EC_{50}) is generally estimated at the end of the exposure
41 duration, meaning that the monitoring of observations over time is not fully exploited. In addition,
42 classical dose-response models implicitly assume that the exposure concentration remains constant
43 all along the experiment, what makes difficult to extrapolate the results to more realistic scenarios
44 with time-variable exposure profiles combining different heights, widths and frequencies of contami-
45 nant pulses (Reinert et al., 2002; Brock, 2009; Jager, 2011; Ashauer et al., 2013). To overcome this
46 gap at the organism level, the use mechanistic models, such as toxicokinetics-toxicodynamics (TKTD)
47 models, is now promoted in order to describe the effects of a substance of interest by integrating
48 the dynamics of the exposure (Jager et al., 2011; EFSA PPR, 2013; Hommen et al., 2016). Indeed,
49 TKTD models appear highly advantageous in terms of mechanistic understanding of the chemical
50 mode of action, of deriving time-independent parameters, of interpreting time-varying exposure and
51 of making predictions under untested situations (Jager et al., 2011; Ashauer et al., 2013). Another of
52 their advantages for ERA is the possible calculation of any $x\%$ lethal $LC(x, t)$ or effective $EC(x, t)$
53 whatever x and at any given exposure duration t . Also, from time-variable concentration profiles as
54 observed in the environment, it is possible to estimate a margin of safety such as the exposure multi-
55 plication factor, $MF(x, t)$, leading to any $x\%$ of effect reduction due to the contaminant at any time
56 t (Ashauer et al., 2013). When focusing on survival rate of individuals, a General Unified Threshold
57 model of Survival (GUTS) has been proposed to unify the majority of TKTD survival models (Jager
58 et al., 2011). In the present paper, we consider the two most used derivations named Stochastic Death
59 (GUTS-RED-SD) and Individual Tolerance (GUTS-RED-IT). GUTS-RED-SD model assumes that all
60 individuals are identically sensitive to the chemical substance by sharing a common internal threshold
61 concentration and that mortality is a stochastic process once this threshold is reached. On the con-
62 trary, GUTS-RED-IT model is based on the Critical Body Residues (CBR) approach, which assumes
63 that individuals differ in their threshold, following a probability distribution, and die as soon as the
64 internal concentration reaches the individual-specific threshold (Jager et al., 2011). The robustness of
65 GUTS models for calibration and prediction has been widely demonstrated in previous studies, with
66 little differences between both GUTS-RED-SD and GUTS-RED-IT models in terms of calibration and
67 prediction (Ashauer et al., 2013; Baudrot et al., 2018c; Jager and Ashauer, 2018). Sensitivity analysis

68 of toxicity endpoints derivated from GUTS, such as $LC(x, t)$ and $MF(x, t)$, have also been investigated
69 (Ashauer et al., 2013; Baudrot et al., 2018c), but the question of how uncertainties are propagated is
70 still under-studied.

71 Quantifying uncertainties or level of confidence associated with toxicity endpoints is undoubtedly a
72 way to improve trust in risk predictors and to avoid decision that could increase, rather than decrease,
73 the risk (Gray and Cohen, 2012; Beck et al., 2016). The Bayesian framework has many advantages to
74 deal with uncertainties since the distribution of parameters, and so their uncertainties, is embedded
75 in the inference process. While the construction of priors on model parameters can be seen as a
76 carrier of subjectivity (Ferson, 2005), there is a proved added-value by taking advantage of information
77 from the experimental design (Delignette-Muller et al., 2017; Baudrot et al., 2018c). Consequently,
78 coupling TKTD models with Bayesian inference allows to estimate the probability distribution of
79 toxicity endpoints, and any other predictions coming from the mechanistic (TKTD) model, by taking
80 into account all the constraints resulting from the experimental design. Moreover, Bayesian inference,
81 which revealed particularly efficient with GUTS models (Delignette-Muller et al., 2017; Baudrot et al.,
82 2018c), can also be used to optimize the experimental design by quantifying the gain of knowledge
83 from priors to posteriors (Albert et al., 2012). At last, Bayesian inference is also tailored for decision
84 making as it confronts the assessors with a range of values, rather than just a point, which is particularly
85 valuable for risk assessment (Ferson, 2005; Gray and Cohen, 2012).

86 In the present study, we explore how scrutinizing uncertainties helps to provide recommendations on
87 the experimental design and the characteristics of toxicity endpoints used for EQS, while maximizing
88 their reliability. We first give an overview of TKTD models with a focus on GUTS (Jager et al.,
89 2011). Handling GUTS models within the R-package *morse* (Baudrot et al., 2018a) is then illustrated
90 with five example data sets. Then, we explore how a variety of experimental designs influence the
91 uncertainties in derived $LC(x, t)$ and $MF(x, t)$. Finally, we provide a set of recommendations on the
92 use of TKTD models for ERA, based on their added-value and the way the uncertainty may be handled
93 under the Bayesian framework.

94 **2. Material and methods**

95 *2.1. Data from experimental toxicity tests*

96 We used experimental toxicity data sets, detailed in (Ashauer et al., 2011; Nyman et al., 2012;
97 Ashauer et al., 2016) testing all together five chemical compounds (carbendazim, cypermethrin, dimethoate,
98 malathion and propiconazole) on the survival rate of the amphipod crustacean *Gammarus pulex*. Two
99 experiments were performed for each compound, one exposing *G. pulex* to constant concentrations,
100 and the other exposing *G. pulex* to time-variable concentrations (see Table 1). In constant exposure
101 experiments, *G. pulex* was exposed to eight concentrations for four days. In time-variable exposure

102 experiments, *G. pulex* was exposed to two different pulse profiles, consisting in two one-day exposure
 103 pulses with short and longer interval between them.

Table 1: Characteristics of data sets used in the manuscript. The "Profile type" is the type of exposure profiles (constant or time-variable), "Data points" refers to the number of data points in the data set, "Nbr profiles" is the number of profiles in the dataset " N_{init} " is the initial number of individuals in profile, "Nbr days" is the number of days for each experiment, and "Time points per profile" is the number of time points for each time series (each constant profiles consisted in 5 time-points).

Product	Profile type	Data points	Nbr profiles	N_{init}	Nbr days	Time points per profile
Carbendazim	constant	40	8	20	4	5
Cypermethrin	constant	40	8	20	4	5
Dimethoate	constant	40	8	20	4	5
Malathion	constant	40	8	20	4	5
Propiconazole	constant	40	8	20	4	5
Carbendazim	variable	51	4	80	10	[8, 14, 16, 13]
Cypermethrin	variable	61	4	80	10	[10, 18, 18, 15]
Dimethoate	variable	58	4	80	10	[10, 16, 17, 15]
Malathion	variable	70	2	70	22	[35, 35]
Propiconazole	variable	74	4	70	10	[11, 21, 21, 21]

104 2.2. GUTS modelling

105 In the following, we detail the mathematical equations of GUTS models describing the survival rate
 106 over time for organisms exposed to a profile of concentrations of a single chemical product. All other
 107 possible derivations of GUTS models are fully described in (Jager et al., 2011; Jager and Ashauer,
 108 2018). We provide here a summary of GUTS-RED-SD and GUTS-RED-IT reduced models in order
 109 to introduce notations and equations relevant for mathematical derivation of explicit formulations of
 110 the $x\%$ Lethal Concentration at time t , denoted $LC(x, t)$, and of the Multiplication Factor leading to
 111 $x\%$ mortality at time t , denoted $MF(x, t)$.

112 2.2.1. Toxicokinetics

113 We denote $C_w(t)$ the external concentration of a chemical product which can be variable over time.
 114 As there is no measure of internal concentration, we use the scaled internal concentration, denoted
 115 $D_w(t)$, which is therefore a latent variable as described by the toxicokinetics part of the model as
 116 follows:

$$\frac{dD_w(t)}{dt} = k_d(C_w(t) - D_w(t)) \quad (1)$$

117 where $k_d [time^{-1}]$ is the dominant rate constant, corresponding to the slowest compensating process
 118 dominating the overall dynamics of toxicity.

119 As we assume that the internal concentration equal 0 at $t = 0$, the explicit formulation for constant

120 concentration profiles is given by:

$$D_w(t) = C_w (1 - e^{-k_d t}) \quad (2)$$

121 An explicit expression for time-variable exposure profiles is provided in Supplementary Material as
 122 it can be useful for implementation, but not for mathematical calculus below. The GUTS-RED-SD
 123 and GUTS-RED-IT models are based on the same model for the scaled internal concentration. They
 124 do not differ in the TK part, but in the TD part describing the death mechanism.

125 From the toxicokinetics equation (2), we can easily compute the $x\%$ depuration time, that is the
 126 period of time after a pulse leading to $x\%$ of reduction in the scaled internal concentration:

$$DRT_x = \frac{-\log(x\%)}{k_d} \quad (3)$$

127 2.2.2. Toxicodynamics

128 *Model GUTS-RED-SD:* The GUTS-RED-SD model supposes that all the organisms have the same
 129 internal threshold concentration, denoted z [$mol.L^{-1}$], and that, once exceeded, the instantaneous
 130 probability to die, named $h(t)$, increases linearly with the internal concentration. The mathematical
 131 equation is:

$$h(t) = b_w \max_{0 \leq \tau \leq t} (D_w(\tau) - z, 0) + h_b \quad (4)$$

132 where b_w [$L.mol.time^{-1}$] is the killing rate and h_b [$time^{-1}$] is the background mortality rate.

133 Then, the survival probability along time under GUTS-RED-SD model is given by:

$$S_{SD}(t) = \exp\left(-\int_0^t h(\tau) d\tau\right) \quad (5)$$

134 *Model GUTS-RED-IT:* The GUTS-RED-IT model supposes that the threshold concentration is dis-
 135 tributed among organisms, and that the death is immediate as soon as this threshold is reached. The
 136 probability to die at the maximal internal concentration with background mortality h_b is given by:

$$S_{IT}(t) = \exp(-h_b t) (1 - F(\max_{0 < \tau < t} (D_w(\tau)))) \quad (6)$$

137 Assuming a log-logistic function, we get $F(x) = \frac{1}{1 + (x/m_w)^{-\beta}}$, with m_w [$mol.L^{-1}$] the median
 138 and β the shape of the threshold distribution, what gives:

$$S_{IT}(t) = \exp(-h_b t) \left(1 - 1 / \left(1 + \left(\frac{\max_{0 \leq \tau \leq t} (D_w(\tau))}{m_w} \right)^{-\beta} \right) \right) \quad (7)$$

139 2.3. Implementation and Bayesian inference

140 GUTS models were implemented within a Bayesian framework through *JAGS* (Plummer, 2016)
141 by using the R-package *morse* (Baudrot et al., 2018a). The Bayesian inference methods, choice of
142 priors and parameterisation of MCMC process have previously been fully explained (Delignette-Muller
143 et al., 2017; Baudrot et al., 2018c,a). The joint posterior distribution of parameters was used to
144 predict survival curve under tested and untested exposure profiles, for the calculation of $LC(x, t)$ and
145 $MF(x, t)$, and for the computing of goodness-of-fit measures (see hereinafter). The use of the joint
146 posterior distribution allow to quantify the uncertainty around all these predictions, and therefore the
147 computing of their median and their 95% credible intervals as follow: under a specific exposure profile,
148 we simulated the survival rate over time for every joint posterior parameter set ; then at each time
149 point of the time series, we computed 0.5, 0.025 and 0.975 quantiles, thus providing median and 95%
150 limits.

151 2.4. Measures of model robustness

152 Modelling is always associated with testing its robustness: the robustness in fitting data used for
153 calibration, but also the robustness for predictions on new data (Grimm and Berger, 2016). To evaluate
154 the robustness of estimations and predictions with the two GUTS models, we calculated their statistical
155 properties by means of the Normalized Root Mean Square Error (NRMSE), the Posterior Predictive
156 Check (PPC), the Watanabe-Akaike Information Criterion and the Leave-One-Out Cross-Validation
157 (LOO-CV) (Gelman et al., 2013).

158 2.4.1. Normalized Root Mean Square Error

159 The Root Mean Square Error (RMSE) allows to characterize the difference between observations
160 and predictions from the posterior distribution. With N observations and $y_{i,obs}$ the observed number
161 of individuals ($i \in \{1, \dots, N\}$), then for each estimation $y_{.,j}$ of the markov chain of size M ($j \in$
162 $\{1, \dots, M\}$) resulting from the Bayesian inference, we can define the $RMSE_j$ such as:

$$RMSE_j = \sqrt{\frac{1}{N} \sum_i (y_{i,j} - y_{i,obs})^2} \Rightarrow NRMSE_j = \frac{RMSE_j}{\overline{y_{obs}}} \quad (8)$$

163 Where Normalized RMSE (NRMSE) is given by dividing RMSE with the mean of the observations
164 denoted $\overline{y_{obs}}$. We then have the distribution of the NRMSE from which we returned the median and
165 the 95% credible interval in Table 2.

166 2.4.2. Posterior Predictive Check (PPC)

167 The Posterior Predictive Check consists in comparing replicated data drawn from the joint posterior
168 distribution to observed data. A measure of goodness-of-fit is the percentage of observed data lying
169 within the 95% predicted credible intervals (Gelman et al., 2013).

170 *2.4.3. WAIC and LOO-CV*

171 Information criteria as WAIC and LOO-CV are common measures of predictive precision also used
 172 to compare models. The WAIC is the sum of the log predictive density computed for every points,
 173 to which a bias is added to take into account the number of parameters. The LOO-CV use the log
 174 predictive density estimated from a training subset and applied it on another one (Gelman et al., 2013).
 175 Both WAIC and LOO-CV were computed with the R-package *bayesplot* (Gabry and Mahr, 2017).

176 *2.5. Mathematical definition and properties of $LC(x, t)$*

177 The $LC(x, t)$ makes sense only in the situation of constant exposure profiles (i.e., whatever time
 178 t , $C_w(t)$ is constant). In such situations, we can provide an explicit formulation of the survival rate
 179 over time considering both models GUTS-RED-SD and GUTS-RED-IT. Many software provides an
 180 implementation of GUTS models what facilitate the possibility to compute the $LC(x, t)$ at any time
 181 and any $x\%$ (Jager and Ashauer, 2018). Our Bayesian implementation of GUTS models using the R
 182 language is one of them (Baudrot et al., 2018a).

183 Let $LC(x, t)$ be the lethal concentration for $x\%$ of organisms at any time t , and $S(C, t)$ be the
 184 survival rate at constant concentration C and time t . Then, the $LC(x, t)$ is defined as:

$$S(LC(x, t), t) = S(0, t) \left(1 - \frac{x}{100}\right) \quad (9)$$

185 where $S(0, t)$ is the survival rate at time t when there is no contaminant, which reflects the back-
 186 ground mortality.

187 *2.5.1. GUTS-RED-SD model*

188 The lethal concentration $LC_{SD}(x, t)$ is given by:

$$LC_{SD}(x, t) = \frac{-k_d \ln \left(1 - \frac{x}{100}\right)}{b_w (k_d(t - t_z) - e^{-k_d t_z} + e^{-k_d t})} + \frac{k_d z (t - t_z)}{k_d(t - t_z) - e^{-k_d t_z} + e^{-k_d t}} \quad (10)$$

189 As mention in Supplementary Material, under time-variable exposure, t_z is also variable with time,
 190 while in the case of constant exposure, t_z is exactly $-1/k_d \ln(1 - z/C_w)$. When time increase, the
 191 $LC_{SD}(x, t)$ curve become a vertical line at point z , and when time tends to infinity, the convergence
 192 is:

$$\lim_{t \rightarrow +\infty} LC_{SD}(x, t) = z \quad , \quad \text{with} \quad t_z = \frac{-1}{k_d} \ln \left(1 - \frac{z}{LC_{SD}(x, t)}\right) \quad (11)$$

193 *2.5.2. GUTS-RED-IT model*

194 The lethal concentration $LC_{IT}(x, t)$ is given by:

$$LC_{IT}(x, t) = \frac{m_w}{(1 - e^{-k_d t})^\beta} \sqrt[\beta]{\frac{x}{100 - x}} \quad (12)$$

195 It is then straightforward to see that when t increases, the $LC_{IT}(x, t)$ converges to:

$$\lim_{t \rightarrow +\infty} LC_{IT}(x, t) = m_w \sqrt[\beta]{\frac{x}{100 - x}} \quad (13)$$

196 In the specific case of $x = 50\%$, we get: $\lim_{t \rightarrow +\infty} LC(50, t) = m_w$.

197 *2.5.3. Calculation of the density distribution of $LC(x, t)$*

198 The calculation of $LC(x, t)$ is based on equation (9). Then, using the GUTS models and the
 199 estimates of parameters from the calibration processes, we compute the survival rate without contam-
 200 ination (i.e., the background mortality denoted $S(0, t)$) and a set of prediction of the survival rate over
 201 a range of concentrations (i.e., $S(C, t)$). This process provides the distribution of the $LC(x, t)$ using
 202 equation (9).

203 *2.6. Mathematical definition and properties of the multiplication factor $MF(x, t)$*

204 Contrary to the lethal concentration $LC(x, t)$ used in situations of constant exposure profiles, the
 205 multiplication factor, $MF(x, t)$ can be computed for both constant and time-variable exposure profiles.

206 With the exposure profile $C_w(\tau)$, with τ running from 0 to t , the $MF(x, t)$ is defined as:

$$S(MF(x, t) \times C_w(\tau), t) = S(0, t) \left(1 - \frac{x}{100}\right) \quad (14)$$

207 In the Supplementary Material, we show that the internal damage $D_w(t)$ is linearly related to
 208 the multiplication factor since whatever the exposure profile (constant or time-variable), we get the
 209 following relation:

$$D_w^{MF}(t) = MF(x, t) \times D_w(t) \quad (15)$$

210 where $D_w^{MF}(t)$ is the internal damage when the exposure profile is multiplied by $MF(x, t)$.

211 *2.6.1. GUTS-RED-SD model*

212 The multiplication factor $MF_{SD}(x, t)$ is given by:

$$MF_{SD}(x, t) = \frac{-\frac{1}{b_w} \ln\left(1 - \frac{x}{100}\right) + \int_0^t \max_{0 < \tau < t} (D_w(\tau) - z, 0) d\tau}{\int_0^t \max_{0 < \tau < t} \left(D_w(\tau) - \frac{z}{MF(x, t)}, 0\right) d\tau} \quad (16)$$

213 When the external concentration is constant, we can use the explicit expression of $D_w(t)$ for $C_w(t) =$
 214 C_w , and get:

$$MF_{SD}(x, t) = \frac{-\frac{1}{b_w} \ln\left(1 - \frac{x}{100}\right) + \frac{C_w}{k_d} (e^{-k_d t} - e^{-k_d t_z}) + (C_w - z)(t - t_z)}{\frac{C_w}{k_d} (e^{-k_d t} - e^{-k_d t_{z, MF}}) + \left(C_w - \frac{z}{MF(x, t)}\right) (t - t_{z, MF})} \quad (17)$$

215 where t_z has been previously defined and $t_{z, MF} = \frac{-1}{k_d} \ln\left(1 - \frac{z}{MF(x, t)C_w}\right)$. As for the $LC_{SD}(x, t)$,
 216 the expression of $t_{z, MF}$ prevents to have a whole explicit formulation of $MF_{SD}(x, t)$.

217 2.6.2. GUTS-RED-IT model

218 The multiplication factor $MF_{IT}(x, t)$ is given by:

$$MF_{IT}(x, t) = \sqrt[\beta]{\frac{100 + x \left(\frac{\max_{0 < \tau < t} (D_w(\tau))}{m_w}\right)^{-\beta}}{100 - x}} \quad (18)$$

219 Therefore, from a GUTS-RED-IT model, solving the toxicokinetics part giving $\max_{0 < \tau < t} (D_w(\tau))$ is enough
 220 to find any multiplication factor for any x at any t . When the external concentration is constant, this
 221 maximum is $C_w (1 - e^{-k_d t})$.

222 3. Results

223 3.1. Goodness-of-fit of GUTS-RED-SD and GUTS-RED-IT

224 For all compounds, Table 2 shows that fitting on constant exposure profiles provide better fit than
 225 for time-variable exposure profiles (see also graphics of Posterior Predictive Check in Supplementary
 226 Material), whatever the measure of goodness-of-fit (except with the NRMSE measure of GUTS-RED-
 227 IT on dimethoate). This result could be expected since, as pointed by Table 1, there are always more
 228 time series in data sets with constant exposure profiles. But also, since there are explicit solutions
 229 of differential equations with constant exposure profiles for both models GUTS-RED-SD and GUTS-
 230 RED-IT, the computing process is easier contrary to time-variable exposure profile requiring the use
 231 of a numerical integrator.

232 For validation, whatever the measure of goodness-of-fit, predictions are always better when pa-
 233 rameters are calibrated on data sets with variable exposure profiles to then predict on data set under
 234 constant exposure profiles, than the other way round.

235 Based on Table 2, it is hard to differentiate GUTS-RED-SD from GUTS-RED-IT with the quality of
 236 their fits. At least, we can notice that GUTS-RED-IT model is particularly bad for Carbendazim and
 237 Dimethoate under time-variable exposure profiles. Still under variable exposure profiles, for Malathion

238 and Propiconazole data sets, we can observed a large 95% credible interval for GUTS-RED-IT (see
 239 figures in Supplementary Material). While NRMSE and %PPC tend to better qualified GUTS-RED-
 240 IT, the uncertainty is penalized with Bayesian measures WAIC and LOO-CV. In fact, the percentage
 241 of recovery extracted from a PPC is totally blind to point large credible interval, since it increases
 242 when the credible interval increases.

Table 2: Results of calibration and validation of models GUTS-RED-SD and GUTS-RED-IT for the five chemical compounds: Carbenazim (car), Cypermethrin (cyp), Dimethoate (Dim), Malathion (mal) and Propiconazole (prz). Profiles of exposure concentration are either constant, denoted *cst*, or variable, denoted *var*. The notation *cst* → *var* means that calibration was done on data set of constant exposure and validation was done on data set of time-variable exposure profile (see data set in Table 1). The measures NRMSE, %PPC, WAIC and LOO-CV assess the goodness-of-fit and are fully explained in section 2.4.

Product	Profile	GUTS SD				GUTS IT			
		NRMSE	%PPC	WAIC	LOO-CV	NRMSE	%PPC	WAIC	LOO-CV
Calibration									
car	cst	0.112	100	402.41	403.27	0.124	100	420.11	422.09
cyp	cst	0.095	100	196.37	206.78	0.092	100	188.07	189.09
dim	cst	0.122	97.5	308.94	309.41	0.171	90.0	357.38	358.74
mal	cst	0.090	100	248.87	249.59	0.112	92.5	273.01	273.54
prz	cst	0.102	100	282.03	285.57	0.118	80.0	308.03	314.93
car	var	0.159	82.1	1006.0	1012.1	0.499	32.1	1222.4	1216.4
cyp	var	0.196	91.7	829.04	833.48	0.116	97.2	793.95	801.23
dim	var	0.129	83.3	1224.8	1226.8	0.161	55.6	1357.2	1344.7
mal	var	0.196	97.8	762.58	766.76	0.148	100	908.56	934.80
prz	var	0.164	95.5	951.10	894.02	0.038	97.7	3262.8	1436.2
Validation: data used for parameter calibration → data for prediction and goodness-of-fit									
car	cst → var	0.159	42.9	17709	4578.4	0.148	50.0	12800	4541.0
cyp	cst → var	0.196	91.7	1760.5	1423.5	0.183	88.9	1283.4	1141.0
dim	cst → var	0.129	83.3	1845.7	1685.3	0.199	63.9	1708.7	1628.9
mal	cst → var	0.196	67.4	10162	2610.7	0.169	63.0	1258.5	1286.1
prz	cst → var	0.164	95.5	940.54	900.90	0.176	90.9	894.41	940.74
car	var → cst	0.164	67.5	537.14	537.79	0.228	90.0	437.01	437.01
cyp	var → cst	0.071	82.5	537.62	488.90	0.051	87.5	453.65	378.89
dim	var → cst	0.013	97.5	302.24	302.30	0.157	87.5	389.32	393.68
mal	var → cst	0.053	80.0	470.28	512.86	0.049	90.0	869.45	732.94
prz	var → cst	0.040	77.5	797.60	660.09	0.041	80.0	1661.3	1107.8

243 3.2. Comparison of $LC(x, t)$ with GUTS-RED-SD and GUTS-RED-IT

244 There is no obvious difference between GUTS-RED-SD and GUTS-RED-IT in their goodness-of-fit
 245 nor in the calculation of $LC(x, t)$ along time t or percentage of affected population, x .

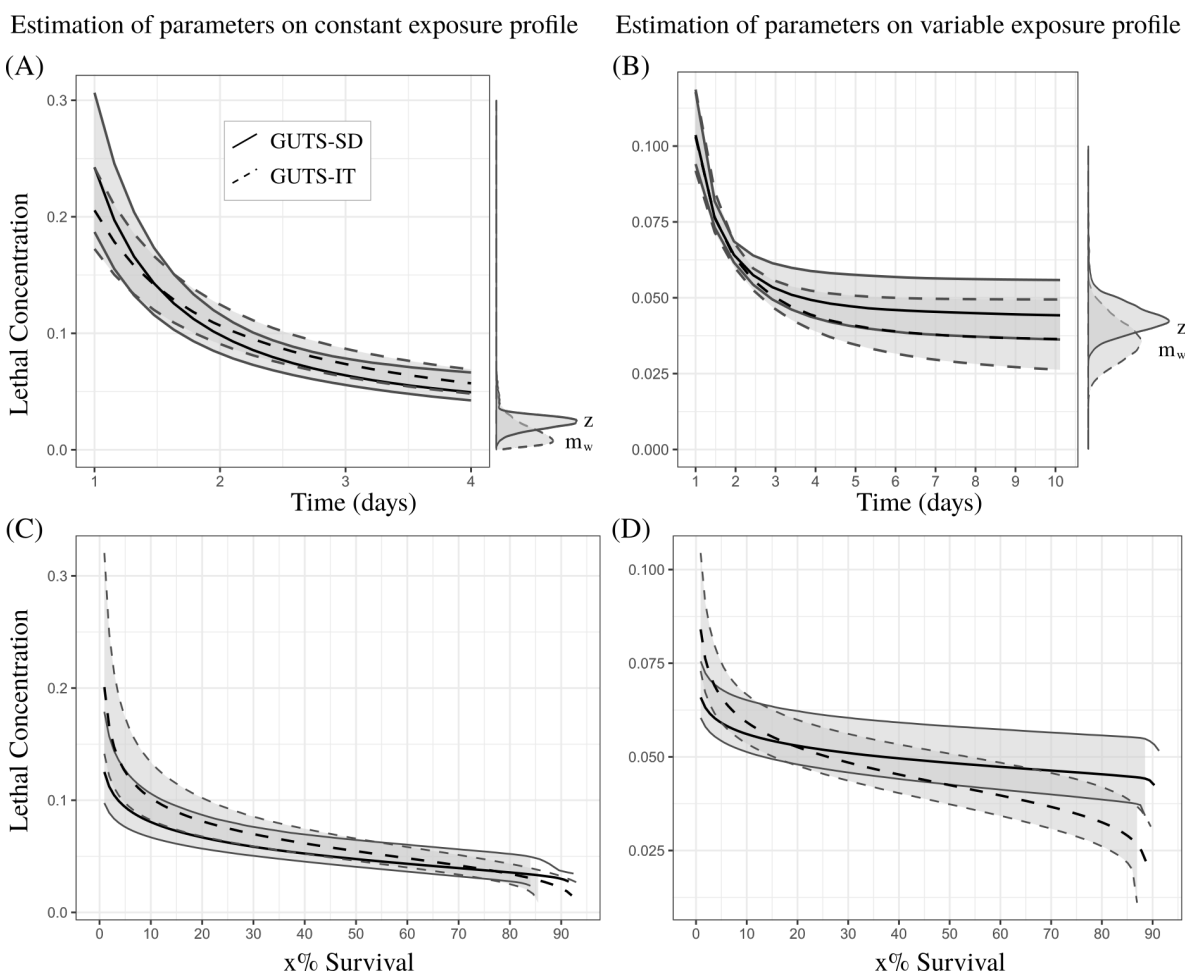


Figure 1: Comparison of $LC(x, t)$ for GUTS-RED-SD, solid lines, and GUTS-RED-IT, dashed lines, for Cypermethrin (see Supplementary Material for other compounds). Parameters are estimated on data under constant (A, C) and variable (B, D) concentration profiles. Black lines are median and grey zones are 95 % credible bands. (A, B) Lethal concentration for 50% of the organisms ($LC(50, t)$) from day 1 to the end of the experiment. (C, D) Lethal concentration at the end of experiment (4 and 10 days respectively) along the percentage of population affected.

246 3.2.1. $LC(x, t)$ as a function of time t

247 As expected, from Figures 1-(A,B) and Supplementary Material, we see that $LC(x, t)$ decreases
 248 with time. Rarely pointed is the shape of this decrease which is exponential and converges toward
 249 different values according to the model. This asymptotic behavior is known as the incipient $LC(x, t)$
 250 (Jager et al., 2006). A direct consequence for risk assessors is that evaluation of $LC(x, t)$ at early time
 251 induces higher uncertainty than at a later time (specific time being relative to the species and the
 252 compound). In other words, the sensitivity of $LC(x, t)$ to time t decreases as long as t increases. For
 253 instance, we see on Figures 1-(A,B) that a little change in time around day 2 leads to a greater change

254 in the estimation of $LC(x, t)$ than around day 4. However, we have to note that the uncertainty of
255 $LC(x, t)$ does not always decreases when time increases. For instance, in Figure 1-(B), the uncertainty
256 at day 6 and afterwards is greater than around day 3.

257 When t increases to infinity, the $LC(x, t)$ converges towards the distribution of parameter z for
258 GUTS-RED-SD (see equation (11)) and $m_w \sqrt{\frac{x}{100-x}}$ for GUTS-RED-IT (see equation (13)). The
259 specific $LC_{50,t}$ tends to z for GUTS-RED-SD and to m_w for GUTS-RED-IT (see equations (11) and
260 (13)). The recommendation for risk assessors would be to use the advantages of TKTD models in order
261 to extrapolate the $LC(x, t)$ on a longer period than the duration of the experiment in order to visualize
262 the uncertainties around the incipient $LC(x, t)$ defined by the asymptote. At least, we recommend to
263 look at the $LC(x, t)$ at the last time of the experiment, what is in line with the common procedure in
264 ERA.

265 3.2.2. $LC(x, t)$ as a function of percentage of affected population, x

266 From Figure 1-(C,D), we can see that the uncertainty of $LC(x, t)$ is greater at low x , that is when
267 the effect of the contaminant is weak. While computing $LC(x, t)$ at $x > 50\%$ is never used for ERA,
268 we can also see that the uncertainty of $LC(x, t)$ increases when x tends to 100%. As a consequence,
269 while the uncertainty is not always minimal at the standard value of $x = 50\%$, it seems to be always
270 smaller around this value than around $x = 10\%$ another classical value used in ERA. Consequently, for
271 risk assessors, while TKTD models allow to compute the $LC(x, t)$ whatever x , if only one value has to
272 be chosen, we recommend to keep the standard of $x = 50\%$. On the other hand, the risk assessor has
273 to keep in mind that 50% is not the optimal threshold in term of reduction of uncertainty, depending
274 on the data set, the model (GUTS-RED-SD or GUTS-RED-IT) and the parameter estimates.

275 3.3. Comparison of $MF(x, t)$ with GUTS-RED-SD and GUTS-RED-IT

276 3.3.1. $MF(x, t)$ as a function of time t

277 As expected, Figures 2-(D-F) show that the multiplication factor is decreasing when the time at
278 which the survival rate is checked increases. In other words, the later the survival rate is assessed,
279 the lower is the multiplication factor. Also, these graphics reveal there is no typical pattern of curves
280 of multiplication factors over time t of exposure. Under a constant exposure profile, the curve shows
281 an exponential decreasing pattern, while under pulsed exposure, we observe a constant phase and,
282 surrounding peaks, a sudden decrease of the multiplication factor. The multiplication factor is ob-
283 viously highly variable around a pulse in the concentration of the chemical product. Therefore, a
284 recommendation would be to wait for some times (e.g., several days) after a peak before computing
285 a multiplication factor. More generally, the multiplication factor is designed to be compared with
286 the assessment factor (AF) classically used in concert with the effect/lethal concentration value based
287 on realistic time-variable exposure profiles to derive an EQS. As a consequence, when using $MF(x, t)$

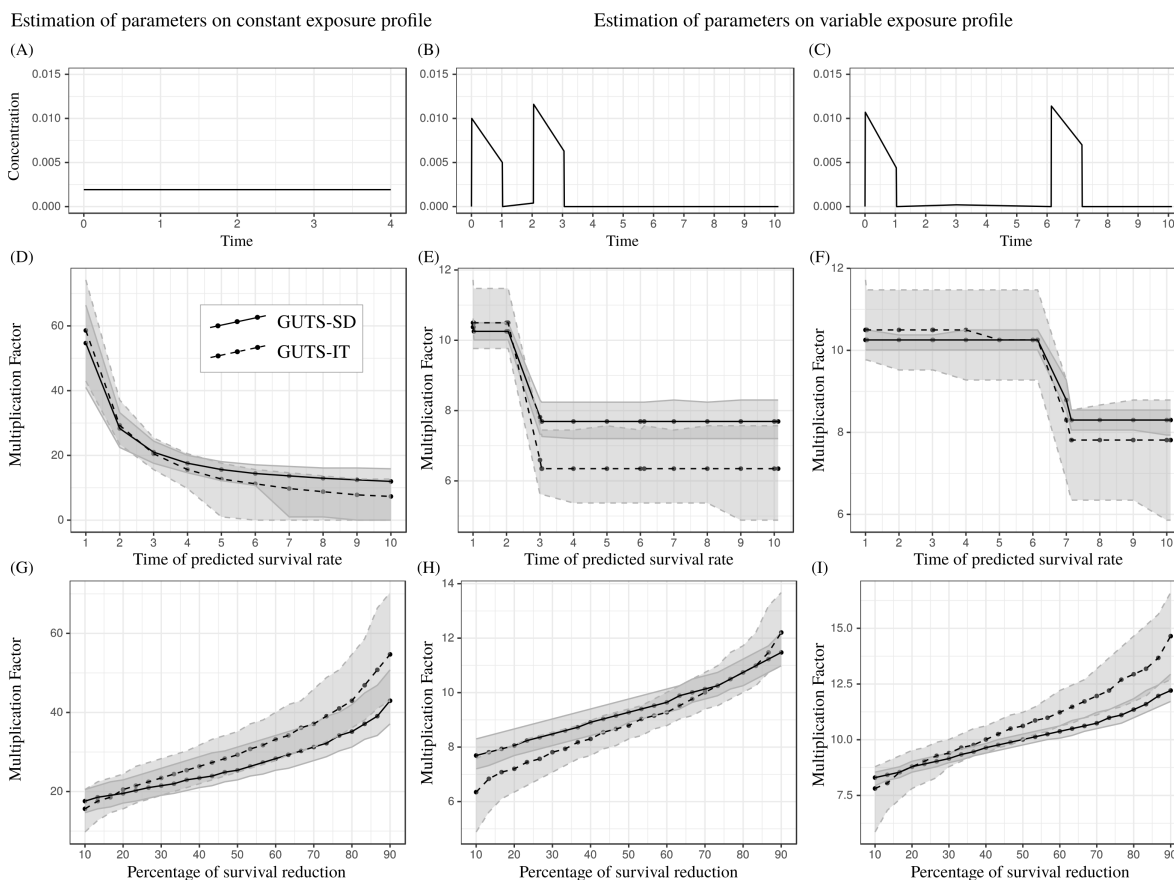


Figure 2: Comparison of $MF(x, t)$ for GUTS-RED-SD, solid lines, and GUTS-RED-IT, dashed lines, for Cypermethrin (see Supplementary Material for other compounds). Parameters are estimated on data under constant (A, D, G) and variable (B, C, E, F, H, I) concentration profiles. (A-C) Exposure profiles, (D-F) Multiplication factors estimated for a 10% reduction of survival (i.e. $MF(x = 10, t)$) along time. (G-I) Multiplication factors estimated at the end of experiments (time 4 for (G) and 10 for (H, I)) along the percentage of survival reduction.

288 based on real exposure profiles, it is important to pay close attention to the amplitudes and frequencies
 289 of pulses, as well as to the times at which multiplication factors are computed. As for the $LC(x, t)$,
 290 taking advantage of TKTD capabilities to predict at any time is of real interest to described the
 291 survival response under pulsed exposure.

292 3.3.2. $MF(x, t)$ as a function of percentage of survival reduction x

293 Logically, Figures 2-(G-I) show that the multiplication factor increases with the increase of the
 294 percentage of reduction of the survival rate. An interesting results is the non-linearity of this increase.
 295 As for the $LC(x, t)$, the uncertainty is greater at low and high percentages compared to what happens
 296 in the middle around 50% of survival reduction. As a consequence, it would be relevant to fix 50% as
 297 a standard for ERA.

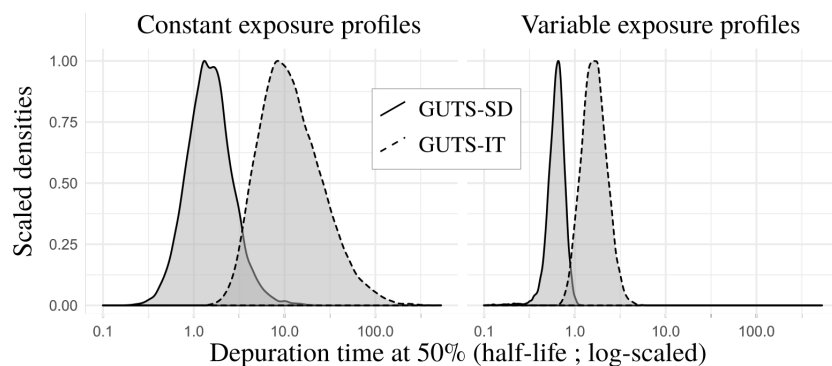


Figure 3: Distribution of estimated half-life for cypermethrin in GUTS-RED-SD and GUTS-RED-IT models for data sets under constant (left) and variables (right) exposure profiles. Median and 95% Credible interval of 50% depuration time are under constant exposure profiles 1.48 [0.502, 5.00] for GUTS-RED-SD and 10.8 [3.21, 68.5] for GUTS-RED-IT, and under variable exposure profiles 0.633 [0.386, 0.890] for GUTS-RED-SD and 1.62 [0.917, 3.06] for GUTS-RED-IT.

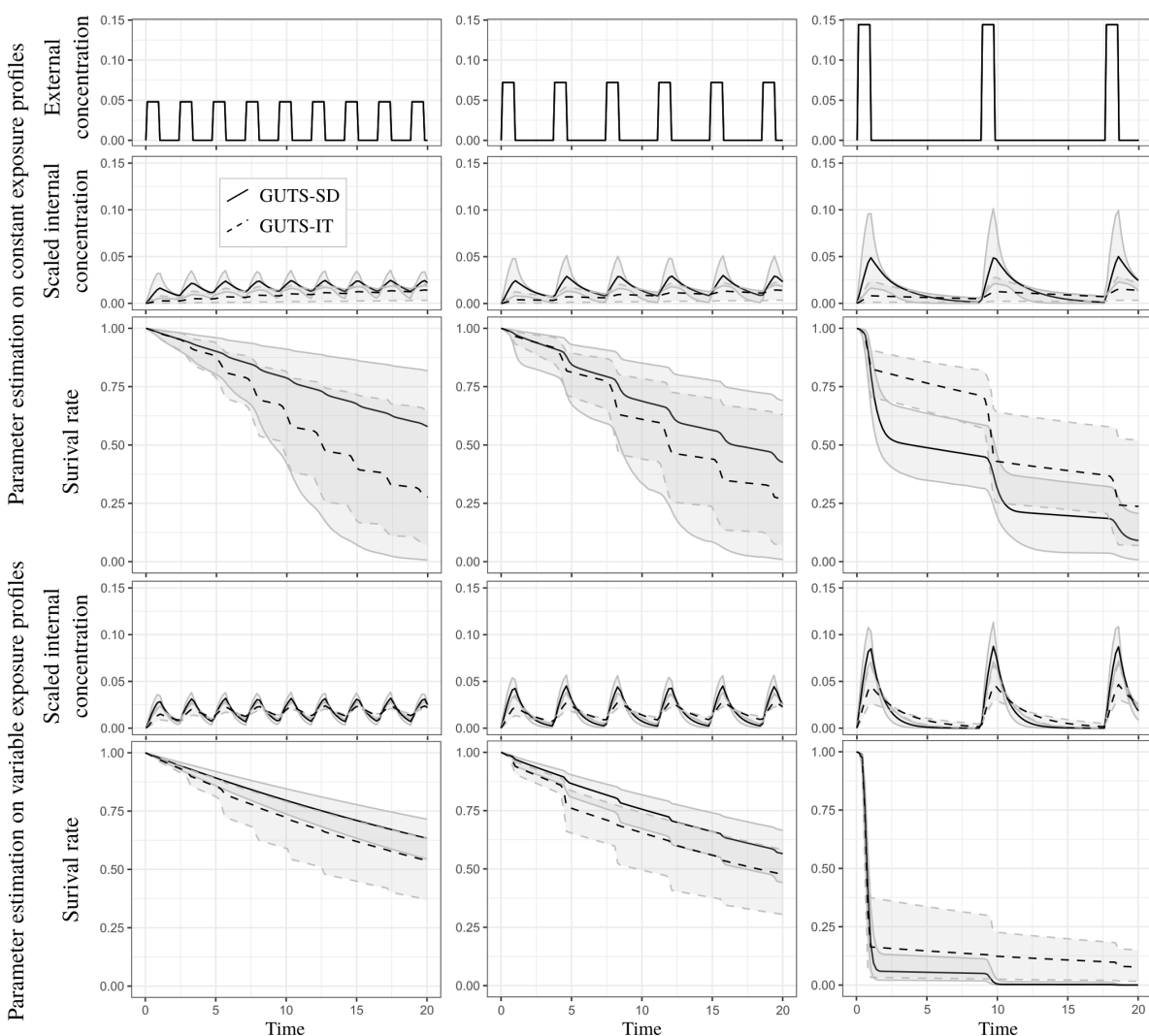


Figure 4: Survival rate over time with GUTS-RED-SD and GUTS-RED-IT models (respectively solid and dashed lines) under different exposure profiles with the same area under the curve (differences are in the duration time after pulses and in the maximal concentration of pulses). Parameters were estimated from the Cypermethrin data set, either under constant (upper panel of the figure) or time-variable (lower panel of the figure) exposure.

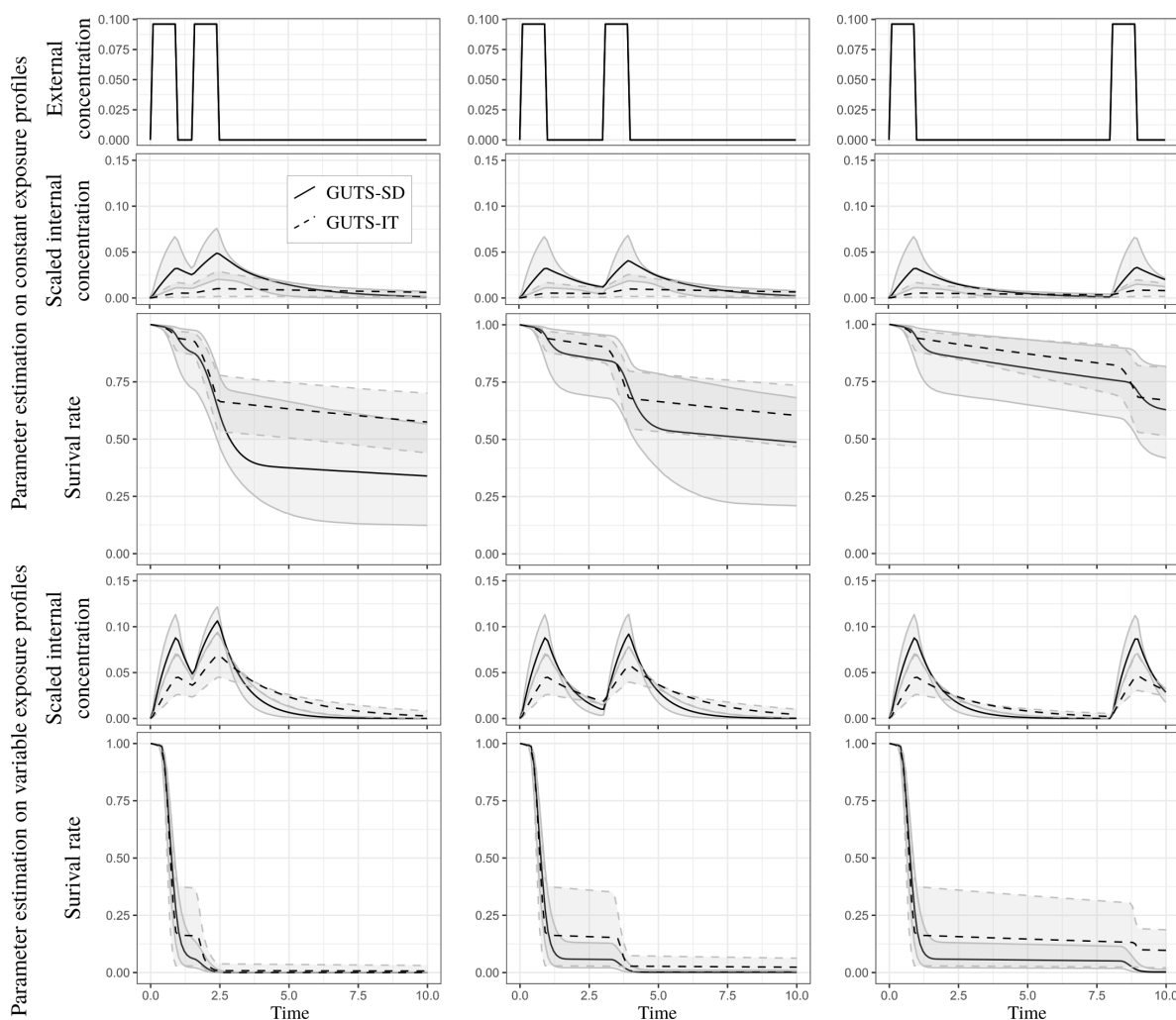


Figure 5: Survival rate over time with GUTS-RED-SD and GUTS-RED-IT models (respectively solid and dashed lines) under two pulsed exposure profile with the same area under the curve (differences are in the duration time between the two pulses). Parameters were estimated from Cypermethrin data set, either under constant (upper panel of the figure) or time-variable (lower panel of the figure) exposure.

298 3.4. Effect of the depuration time on the predicted survival rate

299 3.4.1. Patterns of internal scaled concentration

300 The dominant rate constant, k_d , regulating the kinetics of the toxicant is always greater for GUTS-
 301 RED-SD compared to GUTS-RED-IT, so that the depuration time for GUTS-RED-SD is always
 302 smaller than for GUTS-RED-IT (see Figure 3 and Supplementary Material). As a consequence, un-
 303 der time-variable exposure concentration, the internal scaled concentration with GUTS-RED-SD has
 304 greater amplitude than with GUTS-RED-IT (Figures 4, 5 and Supplementary Material). In other
 305 words, toxicokinetics with GUTS-RED-IT is more smooth than with GUTS-RED-SD. The compen-
 306 sation of the difference in k_d , and therefore in the scaled internal concentration comes from the other
 307 paramaters: threshold z and killing rate k_k for GUTS-RED-SD, and median threshold m_w and shape
 308 β for GUTS-RED-IT. However, the calibration of models being based on the same observed number

309 of survivors, threshold parameter z for GUTS-RED-SD and the median of threshold m_w for GUTS-
310 RED-IT are shifted .

311 *3.4.2. Variation in the number of pulses in exposure profiles*

312 A first step has been to explore the effect of the number of pulses (9, 6 and 3 pulses of one
313 day each) along a period of 20 days with the same cumulative amount of contaminant in external
314 concentration after the 20 days (Figure 4 and Supplementary Material). From a conservative approach
315 for ERA, whatever the model, GUTS-RED-SD or GUTS-RED-IT, it seems better to have few pulses
316 of high amplitude than frequent pulses of low amplitude. Indeed, the survival rate over time with
317 only 3 high pulses is lower than the survival rate under frequent lower exposure. This is confirmed in
318 Supplementary Material for Malathion and Propiconazole data sets. With GUTS mechanistic models,
319 the higher is the pulse, the higher is the scaled internal concentration and so is the damage. Thus,
320 from these simulations, we do not see the effect of the depuration time which could help individual to
321 recover when reducing the frequency of peaks.

322 The comparison between constant and time-variable exposure profiles (Figure 4 and Supplementary
323 Material) suggests that uncertainty is smaller when calibration has been done on data under time-
324 variable exposure profile. The result is counterintuitive, especially since the number of time series
325 was higher with constant exposure profiles what would reduce uncertainties of parameter estimates. If
326 this result is confirmed, then it would be better to predict variable exposure profiles with parameters
327 calibrated from time-variable exposure data sets.

328 *3.4.3. Variation in the period between two pulses*

329 In order to explore the effect of the depuration time, we simulated exposure profiles under two
330 pulses with different time period between them (i.e., 1/2, 2 and 7 days). The cumulative amount of
331 contaminant remains the same for the three simulations. Figure 5 shows that increasing the period
332 between two pulses may increase the survival rate of individuals, whatever the model, GUTS-RED-SD
333 or GUTS-RED-IT. This is a typical result of the depuration period which reduce the level of scaled
334 internal concentration, and therefore reduces the damage. We can easily see that the highest scaled
335 internal concentration is reached when the pulse interval is the smallest. In this situation, we clearly
336 observe the addition of damages from the two pulses. Again, depuration time being different with
337 the two GUTS models, results are also different. For ERA, having two close pulses being the most
338 conservative, we recommend to perform such an experiment. However, the depuration time being
339 the differentiating parameter of GUTS-RED-SD and GUTS-RED-IT, it is also relevant to add an
340 experiment with two pulses separated by a long enough period in order to decorrelate their effect.
341 Thus, having both correlated and uncorrelated experiments, we can better assess the influence of
342 GUTS-RED-SD and GUTS-RED-IT hypothesis on the simulation outputs.

343 4. Discussion

344 4.1. Tracking uncertainties for environmental quality standards

345 Whatever the scientific field, risk assessment is by definition linked to the notion of probability,
346 holding different uncertainties such as the variability between organisms and noises in observations.
347 In this sense, tracking how the uncertainty propagates into models, from collected data to model
348 calculations of toxicity endpoints that are finally used for EQS derivation is of fundamental interest
349 for ERA. For ERA, having good fits over experimental data is not enough. Indeed, the key objective
350 is the application of these fits to predict adverse effects under real environmental exposure profiles,
351 and to derive robust EQS (Laskowski, 1995; Jager, 2011; Gray and Cohen, 2012; EFSA PPR, 2013;
352 EFSA, 2018b). In this context, as we show in this paper, TKTD models calibrated under a Bayesian
353 framework combines two great advantages: on one hand, TKTD models, such as the GUTS models,
354 allow predictions of regulatory toxicity endpoints under any type of exposure profiles ; on the other
355 hand, the Bayesian approach provides the marginal distribution of each parameter, and in this way,
356 allows to track the uncertainty of any prediction of interest.

357 Previous studies investigating goodness-of-fit did not find typical differences between GUTS-RED-
358 SD and GUTS-RED-IT models (Ashauer et al., 2013; Baudrot et al., 2018c). Here again, from the
359 uncertainties in regulatory toxicity endpoints, we do not show evidence to choose GUTS-RED-SD
360 compared to GUTS-RED-IT. A simple recommendation is therefore to use both and then to take the
361 most conservative scenario in terms of ERA. With the 10 data sets we used and the 20 fittings we did,
362 the four measures of goodness-of-fit show similar outputs for both GUTS-RED-SD and GUTS-RED-
363 IT, under both constant and variables exposure profiles. The percentage of observed data lying in the
364 95 % predicted credible interval, denoted $\%PPC$ has the advantage of being linked to visual graphics,
365 PPC plots, and is therefore easier to interpret for risk assessors and stackholders (Beck et al., 2016).
366 However, it may hide a very large uncertainty due to its limitation to 100 % of covering. WAIC and
367 LOO-CV criteria are more robust probability measures (Gelman et al., 2013). Since NRMSE is easy
368 to calculate whatever the inference methods (e.g., Maximum Likelihood Estimation), it could be a
369 relevant measure to check the goodness-of-fit of models.

370 4.2. What about the use and abuse of the lethal concentration?

371 After checking the quality of model parameter calibration, the next question is about the uncer-
372 tainty in toxicity endpoints to derive EQS. Lethal concentrations are nowadays a standard for hazard
373 characterization at levels of 10, 20 and 50 % effect on the population. Many criticisms have been ad-
374 dressed to the lethal and effective concentrations for $x\%$ of the population and other related measures
375 (Jager, 2011). For instance, the classical way to compute the lethal concentration, at the final point,
376 removes information provided by the observations made all along the experiment, and hides the time

377 dependency. For the lethal effect, a classical approach to limit the variability of time duration, is to
378 consider a long enough exposure duration in order to obtain the incipient $LC(x, t \rightarrow +\infty)$ (Jager et al.,
379 2006), that is when the $LC(x, t)$ reaches its asymptote and does not change with increasing duration
380 of exposure as observed on Figure 1. We provide mathematical expression of $LC(x, t)$ convergence,
381 and explicit results when $x = 50\%$ for both GUTS models. We can therefore use the joint posterior
382 parameter distribution provided by the Bayesian inference to compute the distribution the incipient
383 LC .

384 A consequence of the exponential decay of $LC(x, t)$ with increasing time t , is that the uncertainty
385 is greater at early time where a small change in time t induces a great change in the $LC(x, t)$ whatever
386 x . For this reason, classical measures of LC are done at the latest time of experiments. Hence, to
387 compare $LC(x, t)$ of different compounds or species that may require different duration of experiments,
388 using TKTD to extrapolate at other time points is of great advantage. Also, in order to reduce the
389 uncertainty, extrapolation to greater time would be a preferable choice.

390 We show in this study that the uncertainty of $LC(x, t)$ is different according to percentage x under
391 consideration (Figure 1). It appears this uncertainty is limited around 50%, while not specifically at
392 50%, what is in favor of the classical approach to return the LC_{50} . However, it is still of real importance
393 to report the uncertainty of the toxicity endpoints since we show it can drastically change depending
394 on the experimental design, the combination product-species.

395 Among the criticisms of the $LC(x, t)$, one is that it is meaningful only under a set of constant
396 environmental conditions including a constant exposure profile (Jager et al., 2006; Jager, 2011). When
397 the concentration of chemical compounds is highly variable over time in the environment, the use of
398 toxicity endpoints based on toxicity data for constant exposure profiles may hide some processes, such
399 as the response to pulses of exposure. This is the reason underlying the interest of multiplication factor
400 for ERA (Ashauer et al., 2013).

401 4.3. What does it mean to take a margin of safety?

402 The deduction of a margin of safety from a multiplication factor, $MF(x, t)$, quantifies how far the
403 exposure profile is below toxic concentrations (Ashauer et al., 2013). Then, a key question for risk
404 assessors is to target the safest exposure duration, t , and percentage of effect on survival, x . Our
405 study show a lower uncertainty around an x value of 50 %. Thus, to reduce the uncertainty of the
406 $MF(x, t)$ estimation we recommend to select 50%, at least for comparison between studies. We also
407 show that under constant exposure profiles, there is an asymptotic shape of the $MF(x, t)$ as it is for
408 $LC(x, t)$. There is an incipient value of the multiplication factor for any x when t goes to a long
409 time. Therefore, under constant profiles, we could recommend to use the latest time of the exposure
410 profile for toxicity endpoints in order to reduce the sensitivity of the $MF(x, t)$ estimation. However,
411 the $MF(x, t)$ is meaningful when applied on realistic exposure profiles which are rarely constant, and

our study shows that there is no asymptotic shape in such situations. In addition, we observed a great sensitivity of the multiplication factor around peaks in the exposure profiles, that is a high variation of the $MF(x, t)$ with a little change in time t . As a consequence, the assessors has to be very careful about the characteristics of pulses in the exposure profiles in order to understand how they drive changes in the multiplication factor. To do so, we recommend to compute the multiplication factor all along the period of the exposure profile, rather than choosing a single distribution at a specific time.

4.3.1. Depuration time

The survival response to pulses depends on the depuration time driven by the toxicokinetics part of the TKTD model. The kinetics of assimilation and elimination of compounds integrated within the toxicokinetic module is a fundamental part of ecotoxicological models (Wang and Fisher, 1999). In reduced GUTS models, GUTS-RED-SD and GUTS-RED-IT, we assume no measure of the internal concentration, which is therefore calibrated at the same time as other parameters included in the toxicodynamics part. The resulting "scaled internal concentration" is linked to a level of damage defined by the toxicodynamic which has two different hypotheses on the death mechanism for GUTS-RED-SD and GUTS-RED-IT. The mechanistic construction of the model, reflecting biological processes, may be misleading since the toxicokinetic is defined independently of the toxicodynamic part which is chosen afterwards. What is true in the mechanism is not in the inference process where the model parameters, from TK and TD parts, are calibrated all together. As a consequence, as illustrated with our results, the scaled internal concentration does not have the same biological meaning in GUTS-RED-SD and GUTS-RED-IT, and therefore cannot be directly compared between both models.

In both models of course, from the underlying mechanism, we know that damage is positively correlated with pulse amplitude: lower amplitude, lower damage, as we observed from Figure 4. A result is that, with the same cumulative amount of contaminant along an experiment, using fewer pulses reduces final survival rates. So, the most conservative experimental design is the one with fewer pulses of relatively high amplitudes.

Furthermore, from Figure 5, we bring to light the effect of the depuration time. When pulses are close, the organisms do not have time to depurate and therefore there is an addition of the damage and finally a cumulative effect on survival. As a consequence, on a long enough experiment, when pulses become less correlated in terms of cumulative damage, then the final survival rate increases. Because of this, we recommend an experimental design with two close pulses. However, to have a better calibration of the toxicokinetic parameter, it is important to also have two uncorrelated pulses in the experimental design.

Finally, our study reveals that the uncertainty for prediction under time-variable exposure profiles seems to be smaller when calibration was performed with data sets under time-variable rather than under constant exposure profiles. While this observation makes theoretical sense since predictions are

447 made on the same type of profile than calibration of parameters, further empirical studies have to be
448 performed to confirm this point.

449 The environmental dynamics of chemical compounds can be highly variable depending on the whole
450 environmental context (e.g., anthropogenic activities, geochemical kinetics, ecosystem processes) but
451 also on the chemical and bio-transformation of the compound under study. Therefore, as a general
452 recommendation, we would like to point out the relevancy of experimenting several type of expo-
453 sure profiles. Basically, the control and both constant and time-variable exposure profiles including
454 toxicologically dependent and independent pulses seem to be the minimum requirement.

455 *4.4. Practical use of GUTS models*

456 *4.4.1. Optimization of experimental design*

457 The complexity of environmental systems combined with the thousand of compounds produced
458 by human activities implies to assess environmental risk for a huge set of species-compounds combi-
459 nation (Ashauer and Jager, 2018). As a direct consequence, optimizing experimental design in order
460 to maximize the gain of high-quality information from experiments is a challenging requisite, where
461 mechanism-based models combined with the Bayesian approach offer several tools (Albert et al., 2012).
462 A next step of the present study is to use the joint posterior distribution of parameter, and the distri-
463 bution of toxicity endpoints in order to quantify the gain of knowledge of several potential experiments
464 in order to select the most informative. The next objective is thus to develop a framework that could
465 help the construction of new experimental designs in order to minimize their complexity and their
466 number while maximizing the robustness of toxicity endpoint estimates.

467 *4.4.2. Implementation*

468 Although their many advantages, TKTD models, and therefore GUTS models, still remain little
469 used. This is due to their mathematical complexity based on differential equations that need to be
470 numerically integrated when fitted to data (Albert et al., 2016). Associated to their promotion within
471 regulatory documents associated to ERA, the use of GUTS models could be further extended when
472 available within a software environment allowing their handling without immersing into technicalities.
473 Nowadays, several software allow to overpass these difficulties (Jager and Ashauer, 2018; Albert and
474 Vogel, 2017; Baudrot et al., 2018a), and a web-platform is also proposed (Baudrot et al., 2018d).

475 *4.4.3. Limitations*

476 Survival is the most often observed response of a chemical toxic effect in the environment, but
477 sub-lethal effects may be more relevant to manage for ERA, to prevent community collapse (Baudrot
478 et al., 2018b). While the lethal concentration decreases when time increases, other sub-lethal effects
479 (e.g., reproduction, growth) does not always follow this pattern (Álvarez et al., 2006; Jager, 2011).
480 The levels of concentration in acute toxicity tests are higher than those classically observed in the

481 environment. Therefore, under real environmental condition, sub-lethal effects may have more direct
482 impacts on the population dynamics than effects on survival. Thus, it would be of real interest to
483 encompass different effects in a global TKTD approach, in order to better predict when scaling-up at
484 population and community levels (Jager, 2011).

485 Another well-known limitation is the derivation of EQS from specific species-compound combi-
486 nation. In order to extrapolate ecotoxicological information from a set of single species tests to a
487 community, ERA uses Species Sensitivity (Weighted) Distribution, SS(W)D, which can be used to
488 derive EQS covering a set of taxonomically different species (Duboudin et al., 2004). This calculation
489 is classically applied on $LC(x, t)$ and could be easily done with $MF(x, t)$ with the benefit to be applied
490 on time-variable exposure profiles (EFSA, 2018b).

491 4.5. Conclusion

492 As recently written by EFSA experts: "*uncertainty analysis is the process of identifying limitations*
493 *in scientific knowledge and evaluating their implications for scientific conclusions*" (EFSA, 2018a).
494 Description of uncertainties increases transparency and trust in scientific outputs and is therefore a
495 key for an applied science such as ecotoxicology (Beck et al., 2016). Here, we evaluated the combination
496 of mechanism-based models with the Bayesian inference framework to track uncertainties on toxicity
497 endpoints used in regulatory risk assessment from one compound-one species survival bioassay. A lot
498 of other kind of uncertainties emerge all along the decision chain, from the hazard identification to the
499 characterization of risk. Focusing on uncertainty should be of concern at every steps, and above all,
500 for any information returned by mathematical-computational models.

501 Acknowledgement

502 The authors are very grateful for inputs from Theo Brock on an earlier version of the manuscript.
503 The authors also thank the French National Agency for Water and Aquatic Environments (ONEMA,
504 now the French Agency for Biodiversity) for its financial support. The authors declare no competing
505 interests.

506 **References**

- 507 Albert, C., Ashauer, R., Künsch, H., Reichert, P., 2012. Bayesian experimental design for a
508 toxicokinetic–toxicodynamic model. *Journal of statistical planning and inference* 142 (1), 263–275.
- 509 Albert, C., Vogel, S., 2017. GUTS: Fast Calculation of the Likelihood of a Stochastic Survival Model.
510 R package version 1.0.4.
511 URL <https://CRAN.R-project.org/package=GUTS>
- 512 Albert, C., Vogel, S., Ashauer, R., 2016. Computationally efficient implementation of a novel algorithm
513 for the general unified threshold model of survival (guts). *PLoS Comput Biol* 12 (6), e1004978.
- 514 Álvarez, O. A., Jager, T., Redondo, E. M., Kammenga, J. E., 2006. Physiological modes of action
515 of toxic chemicals in the nematode *acroboloides nanus*. *Environmental Toxicology and Chemistry*
516 25 (12), 3230–3237.
- 517 Ashauer, R., Albert, C., Augustine, S., Cedergreen, N., Charles, S., Ducrot, V., Focks, A., Gabsi, F.,
518 Gergs, A., Goussen, B., et al., 2016. Modelling survival: exposure pattern, species sensitivity and
519 uncertainty. *Scientific Reports* 6.
- 520 Ashauer, R., Hintermeister, A., Potthoff, E., Escher, B. I., 2011. Acute toxicity of organic chemicals to
521 *gammarus pulex* correlates with sensitivity of *daphnia magna* across most modes of action. *Aquatic*
522 *toxicology* 103 (1), 38–45.
- 523 Ashauer, R., Jager, T., 2018. Physiological modes of action across species and toxicants: the key to
524 predictive ecotoxicology. *Environmental Science: Processes & Impacts*.
- 525 Ashauer, R., Thorbek, P., Warinton, J. S., Wheeler, J. R., Maund, S., 2013. A method to predict and
526 understand fish survival under dynamic chemical stress using standard ecotoxicity data. *Environ-*
527 *mental toxicology and chemistry* 32 (4), 954–965.
- 528 Baudrot, V., Charles, S., Delignette-Muller, M. L., Duchemin, W., Kon-Kam-king, G., Lopes, C., Ruiz,
529 P., Veber, P., 2018a. morse: MOdelling Tools for Reproduction and Survival Data in Ecotoxicology.
530 R package version 3.0.0.
531 URL <https://cran.r-project.org/web/packages/morse/index.html>
- 532 Baudrot, V., Fritsch, C., Perasso, A., Banerjee, M., Raoul, F., 2018b. Effects of contaminants and
533 trophic cascade regulation on food chain stability: Application to cadmium soil pollution on small
534 mammals–raptor systems. *Ecological Modelling* 382, 33–42.
- 535 Baudrot, V., Preux, S., Ducrot, V., Pavé, A., Charles, S., 2018c. New insights to compare and choose
536 tktd models for survival based on an inter-laboratory study for *Lymnaea stagnalis* exposed to cd.
537 *Environmental science & technology* 52, 1582–1590.

- 538 Baudrot, V., Veber, P., Gence, G., Charles, S., 2018d. Fit guts reduced models online: from theory to
539 practice. *Integrated environmental assessment and management*.
- 540 Beck, N. B., Becker, R. A., Erraguntla, N., Farland, W. H., Grant, R. L., Gray, G., Kirman, C.,
541 LaKind, J. S., Lewis, R. J., Nance, P., et al., 2016. Approaches for describing and communicating
542 overall uncertainty in toxicity characterizations: Us environmental protection agency’s integrated
543 risk information system (iris) as a case study. *Environment international* 89, 110–128.
- 544 Brock, T. C., 2009. *Linking aquatic exposure and effects: risk assessment of pesticides*. CRC Press.
- 545 Delignette-Muller, M. L., Ruiz, P., Veber, P., 2017. Robust fit of toxicokinetic–toxicodynamic models
546 using prior knowledge contained in the design of survival toxicity tests. *Environmental Science &*
547 *Technology* 51 (7), 4038–4045.
- 548 Duboudin, C., Ciffroy, P., Magaud, H., 2004. Effects of data manipulation and statistical methods on
549 species sensitivity distributions. *Environmental Toxicology and Chemistry* 23 (2), 489–499.
- 550 ECHA, 2017. *Guidance on information requirements and chemical safety assessment*.
- 551 EFSA, 2018a. *Guidance on uncertainty analysis in scientific assessments*. *EFSA Journal* 16 (1).
- 552 EFSA, 2018b. *Scientific Opinion on the state of the art of Toxicokinetic/Toxicodynamic (TKTD) effect*
553 *models for regulatory risk assessment of pesticides for aquatic organisms*. *EFSA Journal* (to appear).
- 554 EFSA PPR, 2013. *Guidance on tiered risk assessment for plant protection products for aquatic organ-*
555 *isms in edge-of-field surface waters*. *EFSA Journal* 11 (7), 3290.
- 556 Ferson, S., 2005. *Bayesian methods in risk assessment*. Unpublished Report Prepared for the Bureau
557 de Recherches Geologiques et Minieres (BRGM). New York.
- 558 Gabry, J., Mahr, T., 2017. *bayesplot: Plotting for Bayesian Models*. R package version 1.4.0.
559 URL <https://CRAN.R-project.org/package=bayesplot>
- 560 Gelman, A., Carlin, J. B., Stern, H. S., Dunson, D. B., Vehtari, A., Rubin, D. B., 2013. *Bayesian data*
561 *analysis*. Chapman and Hall/CRC.
- 562 Gray, G. M., Cohen, J. T., 2012. Policy: rethink chemical risk assessments. *Nature* 489 (7414), 27.
- 563 Grimm, V., Berger, U., 2016. Robustness analysis: Deconstructing computational models for ecological
564 theory and applications. *Ecological modelling* 326, 162–167.
- 565 Hommen, U., Forbes, V., Grimm, V., Preuss, T. G., Thorbek, P., Ducrot, V., 2016. How to use mecha-
566 nistic effect models in environmental risk assessment of pesticides: case studies and recommendations
567 from the setac workshop modelink. *Integrated environmental assessment and management* 12 (1),
568 21–31.

- 569 Isigonis, P., Ciffroy, P., Zabeo, A., Semenzin, E., Critto, A., Giove, S., Marcomini, A., 2015. A multi-
570 criteria decision analysis based methodology for quantitatively scoring the reliability and relevance
571 of ecotoxicological data. *Science of the Total Environment* 538, 102–116.
- 572 Jager, T., 2011. Some good reasons to ban ec x and related concepts in ecotoxicology.
- 573 Jager, T., Albert, C., Preuss, T. G., Ashauer, R., 2011. General unified threshold model of survival
574 - a toxicokinetic-toxicodynamic framework for ecotoxicology. *Environmental Science & Technology*
575 45 (7), 2529–2540.
- 576 Jager, T., Ashauer, R., 2018. Modelling survival under chemical stress. A comprehensive guide to the
577 GUTS framework. Version 1.0. Leanpud.
- 578 Jager, T., Heugens, E. H., Kooijman, S. A., 2006. Making sense of ecotoxicological test results: towards
579 application of process-based models. *Ecotoxicology* 15 (3), 305–314.
- 580 Laskowski, R., 1995. Some good reasons to ban the use of noec, loec and related concepts in ecotoxi-
581 cology. *Oikos*, 140–144.
- 582 Nyman, A.-M., Schirmer, K., Ashauer, R., 2012. Toxicokinetic-toxicodynamic modelling of survival of
583 gammarus pulex in multiple pulse exposures to propiconazole: model assumptions, calibration data
584 requirements and predictive power. *Ecotoxicology* 21 (7), 1828–1840.
- 585 Plummer, M., 2016. rjags: Bayesian Graphical Models using MCMC. R package version 4-6.
586 URL <https://CRAN.R-project.org/package=rjags>
- 587 Reinert, K. H., Giddings, J. M., Judd, L., 2002. Effects analysis of time-varying or repeated exposures
588 in aquatic ecological risk assessment of agrochemicals. *Environmental Toxicology and Chemistry*
589 21 (9), 1977–1992.
- 590 Syberg, K., Hansen, S. F., 2016. Environmental risk assessment of chemicals and nanomaterials—the
591 best foundation for regulatory decision-making? *Science of the Total Environment* 541, 784–794.
- 592 Wang, W.-X., Fisher, N. S., 1999. Assimilation efficiencies of chemical contaminants in aquatic inver-
593 tebrates: a synthesis. *Environmental toxicology and chemistry* 18 (9), 2034–2045.